



UNIVERSITÀ
DEGLI STUDI
DI UDINE

Università degli studi di Udine

SIZING AND CONTROL RULES OF DEDICATED MECHANICAL SUBCOOLER IN
TRANSCRITICAL CO₂ BOOSTER SYSTEMS FOR COMMERCIAL REFRIGERATION

Original

Availability:

This version is available <http://hdl.handle.net/11390/1204984> since 2021-07-26T23:40:56Z

Publisher:

Published

DOI:10.1016/j.applthermaleng.2021.116953

Terms of use:

The institutional repository of the University of Udine (<http://air.uniud.it>) is provided by ARIC services. The aim is to enable open access to all the world.

Publisher copyright

(Article begins on next page)

SIZING AND CONTROL RULES OF DEDICATED MECHANICAL SUBCOOLER IN TRANSCRITICAL CO₂ BOOSTER SYSTEMS FOR COMMERCIAL REFRIGERATION

G. Cortella, M.A. Coppola, P. D'Agaro*

DPIA, University of Udine, Italy

paola.dagaro@uniud.it

(*) *Corresponding author*

ABSTRACT

Use of Dedicated Mechanical Subcoolers gives rise to the need of an optimisation process involving gas cooler pressure, activation and setpoint temperature values, subcooling degree and subcooler size, with the aim of further improving the energy efficiency while considering costs.

In this paper a thermoeconomic analysis is performed on a commercial refrigeration plant, at four climate conditions from warm to hot, with time-dependent refrigerating load depending on the location, resulting in some design and control rules for the DMS.

In terms of energy efficiency, the size of the DMS appears to be more crucial at hot climate conditions (difference up to 3.5 % in energy saving), with sizes ranging from 35% to 45% of the total cooling capacity. Optimal control rules should be preferentially adopted at mild-warm conditions, suggesting to exploit the highest subcooling rate available. The economic analysis shows that energy use is the most important cost item.

Keywords: CO₂, Commercial refrigeration, Subcooling, Optimization, Cost

NOMENCLATURE

General

A	Area	[m ²]
c	Specific cost	[€/kW]
C	Cost	[€]
COP	Coefficient Of Performance	[-]
CRU	Commercial Refrigeration Unit	
DMS	Dedicated Mechanical Subcooling	
e	Cost percentage factor	
f	Actualization factor	
GC	Gas Cooler	
GWP	Global Warming Potential	
i	interest rate	
HS	High Stage	
LS	Low Stage	
LT	Low Temperature	
MT	Medium Temperature	
m	Mass	[kg]
\dot{m}	Refrigerant flow rate	[kg/s]
p	Pressure	[bar]
Q	Heat flow	[kW]

t	Temperature	[°C]
w	Specific compressor work	[kJ/kg]
W	Compressor power	[kW]
Δh_{sub}	Subcooling degree, enthalpy	[kJ/kg]
Δt_{sub}	Subcooling degree, temperature	[K]
Δp_{GC}	DMS reduction in gas cooler pressure	[bar]

Subscripts/Superscripts

act	activation
app	approach
ext	external/outdoor
$evap$	evaporator
el	electricity
GC	Gas Cooler
HS	High Stage
LS	Low Stage
LT	Low Temperature
MT	Medium Temperature
m	maintenance
max	maximum
opt	optimal
rec	receiver
ref	refrigerant
set	setpoint
sub	subcooling, subcooled refrigerant
tot	total

Greek symbols

α	DMS to main cycle cooling capacity ratio (Eq. 7)
β	Compression ratio
η	Compressors' efficiency
φ	Flow rate ratio parameter (Eq. 4)
ψ	Vapour quality complementary parameter

1. INTRODUCTION

The employment of natural refrigerants, in particular for commercial refrigeration, has been promoted as a long term solution to face global warming. In fact, the Kigali amendment to the Montreal Protocol and, in Europe, the EU regulation 517/2014 on fluorinated greenhouse gases force a phase down schedule for the hydro-fluorocarbons.

Carbon dioxide, due to its characteristics such as low Global Warming Potential (GWP = 1) and high safety features (A1 ASHRAE classification, non-toxic and non-flammable), is one of the most promising natural working fluids in the commercial refrigeration sector. Furthermore, supermarket refrigeration systems employ large amounts of refrigerant and have a large direct environmental impact related to refrigerant leakage, thus CO₂ even more so than ever reveals to be one of the best candidates.

However, although CO₂ systems perform well at subcritical condition, in transcritical regime they suffer significant reduction of the efficiency. Transcritical operation occurs for warm and hot outdoor temperature, thus it is a characteristic of warm and hot climates. In order to improve the performance in transcritical regime and thus extend the convenience of use of CO₂ in warm climates, many efforts have been made, especially in

the last decades. Several technologies and alternative plant schemes have been studied and tested, showing that improvements of the performance in CO₂ refrigeration plants can be achieved.

As a result, CO₂ direct expansion systems are currently popular solutions for commercial refrigeration and the number of stores using CO₂ transcritical refrigeration technology has been increasing substantially all over the world, especially in Europe, where 29000 installations are reported in May 2020 with a 81 % growth from 2018 to 2020 [1].

One of the most recently investigated and promising solution, among the several ones available, is Dedicated Mechanical Subcooling (DMS), that consists in subcooling the refrigerant exiting the gas cooler by means of a separated refrigerating unit. This has the effect of increasing the available cooling capacity corresponding to a given compression work in standard cycle. When it comes to booster systems, subcooling strategy reduces the amount of flash gas produced at the liquid receiver.

This solution appears to be recommended particularly at high outdoor temperature, and natural fluids like R-290 are becoming widespread for environmental safety reasons [2, 3].

Llopis et al. [4] have collected in their review manuscript a number of papers which witness the effectiveness of the DMS solution in various system configurations, concluding that optimum conditions (subcooling degree and optimum high pressure) have not been extensively investigated, and that a thermoeconomic approach would be needed to reach definite conclusions. Llopis et al. themselves [5] simulated both single and double stage CO₂ plants with a R-290 DMS, predicting efficiency increase up to 20 % while reducing the gas cooler pressure of up to 12 bar when using DMS in a booster cycle at -30 °C evaporating temperature and 35 °C outdoor temperature. They performed tests on a small (4 kW) single stage double-throttling CO₂ refrigerating plant with a 0.7 kW R-1234yf DMS, and found a COP increase of around 23% at 0°C evaporating temperature and 30.2 °C gas-cooler exit temperatures [6], and found that the gas cooler pressure could be reduced up to 8 bar [7]. A similar experimental work has been performed on the same plant with R-152a in the DMS by Nebot-Andres et al. [8] to determine optimum operating conditions and give correlations for the gas cooler pressure and subcooling degree. Dai et al. [9] too investigated theoretically the optimum conditions for various refrigerants for the DMS, finding an increase in COP up to 25% at 0°C evaporating temperature and 30 °C outdoor temperature. The best results are achieved with R-717, but with a pretty small advantage with respect to other non-toxic however flammable fluids like R-290 or R-E170, or mildly flammable with low GWP like R-152a and HFOs R-1234ze and R-1234yf. Instead, the effect of sudden changes in capacity for a CO₂ transcritical booster cycle with mechanical subcooler have been investigated by Bush et al. [10]. Through modelling and performing lab tests they identified some interactions between load sheds at the MT and LT levels and power reduction, considering the effect of the subcooler, and underlining the importance for further investigations.

Many authors applied economic and exergoeconomic analysis to the energy assessments of systems including CO₂ refrigerating cycles. Mosaffa et al. [11] carried out exergoeconomic and environmental analyses for two different CO₂/NH₃ cascade refrigeration systems: system 1 with two flash tanks and system 2 with a flash tank and a flash intercooler with an indirect subcooler. In their evaluation, the authors included also the cost rate due to greenhouse gas emission, considering a number of operating variables. The results of such analyses demonstrate the benefits and profitability given by the two systems, and identify the operating conditions at which the minimum annual total cost rate is obtained, which are different from those at which the maximum COP and exergy efficiency are obtained. In this way they identify the component with dominating investment, operating and maintenance cost.

An energy, exergy and exergoeconomic analysis was performed by Gullo et al. [12] with reference to CO₂ systems, to evaluate the benefits of parallel compression also from an economic point of view, and concluding that, in spite of the extra investment cost, the new configuration allows a 6.7 % saving in the total cost on a 15 years lifetime basis. In this case, energy and economic benefits are in agreement.

Another energetic, exergetic and exergoeconomic assessment has been proposed by Dai et al. [13], for a transcritical CO₂ reversible heat pump, integrated with DMS, aimed to residential heating and cooling applications, in several climates. The performance of the system has been compared to a baseline CO₂ system without DMS. They conclude that the COP and seasonal performance can be improved with the DMS by up to around 38% and 23% respectively, and the latter generally increases with the reduction in latitude. Moreover, exergy efficiency with DMS

is higher, of around 25%, and declines with latitude. From a thermoeconomic point of view, the introduction of the DMS is appeared to be cost effective, with a total cost reduction of about 17%. The exergoeconomic factor showed to increase with an improvement of the building thermal insulation and reduces with the compressor price reduction.

Furthermore, in a previous work, still Dai et al. [14] carried out an investigation where DMS is employed to improve the operation characteristics of transcritical CO₂ heat pump for residential space heating. Energy, exergy and economic methodologies are applied to study the performance of the system at five typical Chinese climate regions, with different heating terminals. The results showed that when using a DMS, with an optimum discharge pressure and subcooling degree, the COP shows an improvement of the order of 25%. In severe cold regions, the seasonal integrated energy efficiency can be enhanced by 32%, using floor-coil radiator or normal fan-coil units. The optimal subcooling degree is relatively large (21–39 °C), while the power consumption ratio between the DMS and the CO₂ system is rather small (0.22–0.36). The introduction of DMS also improves the exergy efficiency of the system. The total capital investment and electricity cost resulted to be both lower than that of traditional CO₂ heat pump for residential heating. The levelized annual total cost can be reduced by 7.5–15.3%. The cost of the DMS subsystem appeared low compared with the CO₂ system (about 4% of the total capital cost).

Regarding the economic analysis of CO₂ refrigerating systems, also their application in complex systems for cogeneration and trigeneration has been investigated. Mohammadi et al. [15] provided a thorough thermoeconomic evaluation to demonstrate that waste energy recovery from refrigeration cycles would be useful to produce several outputs for cogeneration and trigeneration applications. The results showed that a significant amount of cooling capacity for air conditioning and refrigeration purposes can be obtained by means of a water-lithium bromide absorption or ammonia-water absorption chiller, recovering heat discarded from the CO₂ main refrigeration cycle. This fact offers the chance to use such cooling capacity for subcooling purposes, thus increasing the COP of the main cycle.

Coupling CO₂ refrigeration plants to air conditioning systems has also been investigated widely, mostly from an energy point of view. In the view of performing subcooling, Cortella et al. [16, 17] simulated the operation of a system where the subcooling demand can be provided by an HVAC system, when this is available. This solution has showed lower performance with respect to DMS, but it can give rise to an economic advantage thanks to its low investment cost.

In this work, in the first place, an energy analysis has been carried out aiming to establish which is the best combination of parameters that affect the functioning of the CO₂ transcritical booster system with DMS, in order to maximize the plant overall performance. How the global COP is related to all the system variables has already been investigated in a previous work by D'Agaro et al. [18], where a COP correlation has been sought for the plant under a fixed domain of the parameters. In this work the domain has been extended in order to cover a wider range of some parameters, first of all the subcooling degree, and to include new variables such as the subcooler activation temperature and the subcooler set point temperature. The computations have been performed by means of a comprehensive model built in the Trnsys environment [19], which includes the transcritical CO₂ booster refrigeration unit, as well as the display cabinets and cold rooms [20, 21], and a R-1234yf DMS unit. The model has been calibrated and validated against the field data gathered during a whole year from the monitoring of an actual refrigerating system in operation in a small sized supermarket located in Northern Italy as described by Cortella et al. [22] and D'Agaro et al. [23]. The optimal operating conditions of the system are identified, and the energy saving produced by the control of the gas cooler pressure, as a function of the subcooling degree and the outdoor temperature, has been estimated, along with the analysis of the influence of the size of the subcooler and the activation and set temperatures of the DMS. In fact, the latter determines a wide span of the evaporating levels achieved in the DMS that in turn affects the COP of the DMS itself, and of course of the entire system. Simulations are carried out on an annual basis, with hourly time step, for four exemplary climatic conditions, from warm to hot. As a further improvement with respect to previous works [17, 18], both the LT and MT cooling load profiles are estimated separately at each climate hour by hour considering the internal air temperature which on turn results from the dynamic thermal building simulation at the different outdoor conditions. This is a peculiarity of this work, and at the best of our knowledge no research has been done on this regard. In fact, all comparisons among different plant configurations are usually performed at constant cooling load. Finally, a simple cost analysis is applied for the

first time, at the best of author's knowledge, to the implementation of DMS, where the investment costs are calculated for a lifecycle of 10 years, in order to check if the most energy-effective solutions are also cost-effective.

2. SYSTEM AND MODEL

The commercial refrigeration plant considered in this work is a transcritical CO₂ booster system, feeding closed refrigerated display cabinets, both for chilled and frozen food, that has been monitored for over a year in a small supermarket of approximately 1200 m², located in northern Italy. The peak cooling capacity of display cabinets and cold rooms is equal to 39.7 kW for the Medium Temperature (MT) level and to 6.8 kW for the Low Temperature (LT).

Every component of the refrigeration system has been described by in-house mathematical models developed in the TRNSYS environment and validated under all the possible operating conditions (mainly divided into subcritical, transition and transcritical). The model allows to carry out simulations with time dependent input variables and has the capability to store in time the residual cooling energy given by the activation statuses of the compressors that may exceed the cooling demand from refrigerated display cabinets. The description of the DMS and its interaction with the refrigeration system is also integrated in the model.

The transcritical CO₂ booster cycle has a liquid receiver and flash gas expansion valve. *CoolProp* libraries [24] are linked to our in-house routines in the TRNSYS environment to estimate the refrigerant properties in the thermodynamic cycle; the instantaneous mass flow rate is calculated in order to satisfy the cooling capacity estimated by the time dependent models of the display cabinets and cold rooms, and it defines the status of the compressor racks; the compressors themselves have been described using the manufacturer correlations.

The detailed description of the refrigerating system, including information on the configuration of the LS and HS compressor racks and activation rules, is given in D'Agaro et al. [23], where a thorough calibration and validation process of the model and control rules has been carried out against the yearly field data available from the real plant. The plant layout with DMS and the thermodynamic cycle in a (*p-h*) chart are given in Fig. 1, while the values of the main design parameters and settings are recalled in Table 1.

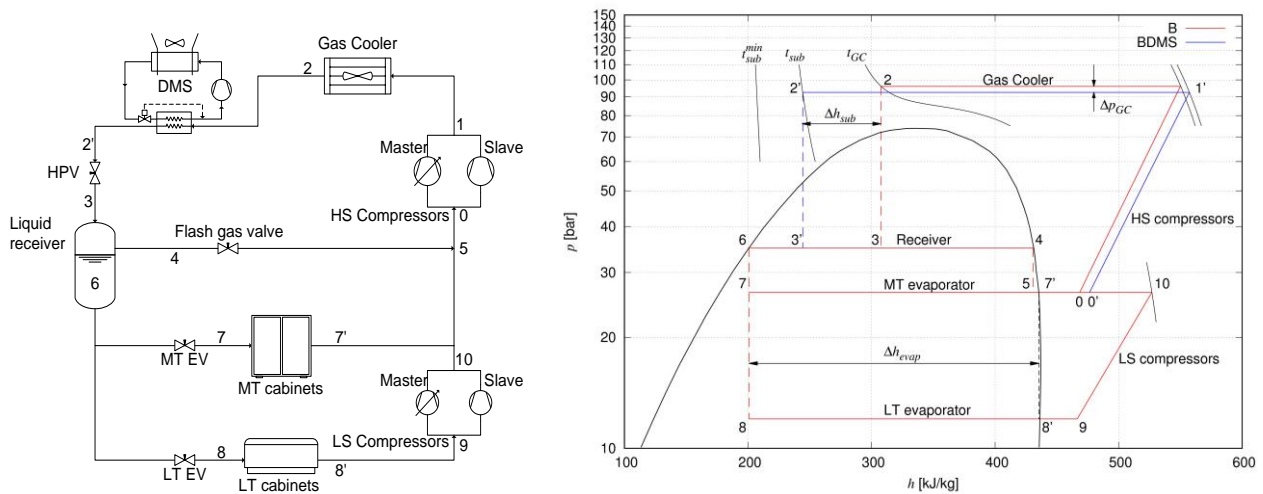


Figure 1: CO₂ booster refrigeration system with DMS: schematic drawing (left); thermodynamic cycle in a (*p-h*) diagram without (B) and with (BDMS) Dedicated Mechanical Subcooling

The superheating values reported in Table 1 and considered in the model come from experimental values recorded at the supermarket plant. They are due to heat loss in the long suction lines from the cabinets to the machine room. We considered such high values in order to perform comparisons at the most realistic operating conditions of the plant. No useful superheating in the evaporators has been considered for a conservative evaluation of the COP. The plant has the possibility of subcooling the refrigerant at the exit of the gas cooler by means of a Dedicated Mechanical Subcooler (DMS), that consists of a single-stage cycle working with R-1234yf as refrigerant. This fluid has been chosen among other flammable natural refrigerants like R-152a and

propane, isobutane, or propylene, thanks to its non-toxicity when compared to ammonia and low flammability (A2L) when compared to hydrocarbons (A3) and considering that it offers a remarkably low global warming potential ($GWP_{100} < 1$) when compared to R-152a, even if this last fluid has slightly better performance and lower cost, but might be subject to restrictions in the near future ($GWP_{100} = 138$) [25].

The effects of subcooling on the CO₂ cycle are depicted in Fig. 1 compared to the basic cycle, the subcooling (Δh_{sub}) reduces the exit temperature at the high stage pressure and lowers the vapour quality at the receiver, with the effect of reducing the amount of flash gas produced.

The thermodynamic cycle of the subcooler unit has been modelled according to the parameter values reported in Table 1 (DMS unit) and taking into account the compressor operating limits. Standalone simulations have been carried out in order to infer the COP as a continuous function of the outdoor temperature and evaporating level, i.e:

$$COP_{DMS}(t_{ext}, t_{evap,DMS}) = a_1 t_{ext}^3 + a_2 t_{evap,DMS}^3 + a_3 t_{ext}^2 + a_4 t_{evap,DMS}^2 + a_5 t_{ext} + a_6 t_{evap,DMS} + a_7 t_{ext}^2 t_{evap,DMS} + a_8 t_{ext} t_{evap,DMS}^2 + a_9 t_{ext} t_{evap,DMS} + a_{10} \quad (1)$$

$$\begin{aligned} a_1 &= -4.3234 \cdot 10^{-5} & a_2 &= 9.2930 \cdot 10^{-5} & a_3 &= 3.9065 \cdot 10^{-3} & a_4 &= 4.2568 \cdot 10^{-3} & a_5 &= -2.2530 \cdot 10^{-1} \\ a_6 &= 2.0343 \cdot 10^{-1} & a_7 &= 1.4998 \cdot 10^{-4} & a_8 &= -1.9838 \cdot 10^{-4} & a_9 &= -7.7066 \cdot 10^{-3} & a_{10} &= 7.6353 \end{aligned}$$

It ranges from 1.4 to 4.4 at the minimum evaporating level $t_{evap,DMS}$ (0°C) for the outdoor temperature t_{ext} from 20°C to 46°C and from 3.5 to 5.5 for the minimum evaporating level (20°C) in the same outdoor temperature [18]. In Eq. (1), temperature values are in °C.

The coupling between DMS and booster system reflects an ideal condition, where the evaporating temperature of the DMS can follow the temperature fluctuations at the exit of the gas cooler, which in turn depend on the cooling load, outdoor temperature, gas cooler fans operation. This coupling is implemented as follows:

- The evaporating temperature of the DMS cycle $t_{evap,DMS}$ is set at:

$$t_{evap,DMS} = \max [(t_{sub,set} - \Delta t_{app,DMS}); t_{evap,DMS,lim}] \quad (2)$$

- where $t_{sub,set}$ is the set point value for the temperature at the exit of the subcooler, $\Delta t_{app,DMS}$ is the minimum evaporator approach temperature (values in 1) and $t_{evap,DMS,lim}$ is imposed, for a given condensing temperature, by the compressor operating limits. Once the evaporating level has been fixed and the DMS size is known, a check is carried out to verify if the outdoor temperature and the available DMS cooling capacity allow to reach the set point temperature $t_{sub,set}$, otherwise the achievable CO₂ exit temperature t_{sub} is calculated.
- Finally, when the effective t_{sub} is defined, and thus the subcooling degree, for a certain outdoor condition and demand of cooling capacity it is possible to impose the optimal values of the gas cooler pressure in transcritical mode. In this way the COP of the overall system (CO₂ booster plus subcooler) is maximized.

The procedure followed to optimize the overall system is described in the next section.

Table 1. Main design parameters for the CO₂ booster System (B) and for the DMS unit.

CO₂ booster System			
Symbol	Parameter	Unit	Value
	LT evaporating temperature	°C	-35
	MT evaporating temperature	°C	-10
	Minimum condensing temperature at subcritical conditions	°C	6
P_{rec}	Liquid receiver pressure	bar	35
	Subcooling at subcritical conditions	K	3
	Gas Cooler/Condenser approach temperature difference	K	4

	LT superheating (up to experimental suction temperature)	K	30
	MT superheating (up to experimental suction temperature)	K	20
	LS compressors	Bitzer 2JSL-2K Bitzer 2KSL-1K	
	HS compressors	Bitzer 4FTC-20K Bitzer 4JTC-15K	
$t_{DMS, act}$	outdoor temperature for subcooler activation	°C	(19, 22, 25)
$t_{sub, set}$	temperature set for CO ₂ at the subcooler outlet	°C	(5, 10, 15, 20)

DMS unit – Refrigerant R-1234yf

	<i>Parameter</i>	<i>Unit</i>	<i>Value</i>
$\Delta t_{app,DMS}$	Evaporator approach temperature (minimum value)	K	5
	Condenser approach temperature	K	10
	Superheating	K	10
Q_{DMS}	Cooling capacity	kW	(11.6 – 23.5)
α	DMS to main cycle cooling capacity ratio	%	25 – 50, <i>step</i> = 5
η_{DMS}	Compressor global efficiency (scroll type)	$\eta_{DMS} = -0,07\beta^2 + 0.4796\beta - 0.1234$	

3. PARAMETER SETTING AND OPTIMAL CONDITIONS

It is well known that the heat rejection pressure at the gas cooler, in a transcritical cycle, is a free parameter, unlike subcritical cycles, and normally an optimum value is always sought in order to operate the system in an efficient way. Nevertheless, when it comes to integrate refrigeration systems with DMS, the quest for a function of the optimum gas pressure is not trivial. Many authors have studied the behaviour of the COP of subcooled transcritical systems, and analysed how the optimum gas cooler is related to other parameters. In particular, for a booster system with two evaporating levels, an analysis of the COP has been carried out in D'Agaro et al. [18], where they showed that the global COP of the system has the following expression:

$$COP = \frac{\Delta h_{evap}}{\varphi w_{LS} + \frac{1}{\psi} \left(w_{HS} + \frac{\Delta h_{sub}}{COP_{DMS}} \right)}. \quad (3)$$

This equation contains the main parameters such as: Δh_{evap} , that is the evaporating enthalpy, which is pretty much the same at the two levels LT and MT (Fig.1); the specific work w of the two compressor stages LS and HS, that is an intrinsic behaviour of the compressor model, described by the manufacturer's polynomials; the COP of the DMS, normally a function of the outdoor and evaporating temperatures (Eq. 1); the non-dimensional parameter ψ , which is the complementary to the vapour quality at the receiver inlet, therefore this quantity measures the amount of flash gas produced; the non-dimensional parameter φ defined as:

$$\varphi = \frac{\dot{m}_{LT}}{\dot{m}_{LT} + \dot{m}_{MT}}. \quad (4)$$

When a DMS unit is in use in a booster system, the subcooling has basically the effect of lowering the amount of flash gas at the receiver (status 3 shifts to 3' in Fig. 1) while, keeping the intermediate pressure constant, the specific cooling capacities at the two evaporating levels do not change (same status 6 in Fig. 1). Thus, the power elaborated by the high stage compressors is reduced as the mass flow rate of flash gas decreases.

If specific quantities are considered, as in Eq. (3), the benefit, which is still on the reduction of the high stage electrical power, can be explained by the increase of ψ and the reduction of w_{HS} . Obviously, the better the COP of the DMS the higher is the global COP of the system.

As the parameter φ is concerned, higher values of φ are given by higher cooling loads at the LT, with the effect of penalising the COP. In a previous work [18] the effect of φ on the plant performance has been investigated, in the present paper the parameter is kept constant and equal to the yearly averaged value 0.176 for the considered plant.

Once the plant operating conditions are defined (i.e. the parameters of Table 1 and the φ value), the COP in Eq. (3) essentially depends on three variables:

$$COP = f(p_{GC}, \Delta h_{sub}, t_{ext}) = f(p_{GC}, \Delta t_{sub}, t_{ext}) \quad (5)$$

namely the gas cooler pressure p_{GC} , the subcooling degree Δt_{sub} , and the heat rejection temperature (outdoors) t_{ext} which is intended for both the booster and DMS cycle.

In this work, the validity domain of the subcooling degree Δt_{sub} has been extended reaching values up to almost 40 K, as low set points of the subcooler exit temperature and higher external temperature are considered.

Simulations have been carried out in order to obtain the global COP of the overall system for all combinations of the parameters in equation (5), each one in their own domain, in particular: the outdoor temperature t_{ext} ranges, in transcritical mode, from 26°C to 40°C with a 1 K step, p_{GC} ranges between 75 bar and 110 bar with a 0.5 bar step and Δt_{sub} with a 1 K step, varies between the lowest value of 1 K and the highest value achievable that depends on t_{ext} and $t_{sub,set}$, the latter equal to the minimum value of 5°C.

This procedure permits to identify the couple of controllable variables $(p_{GC}, \Delta t_{sub})_{opt}$ that maximizes the COP in transcritical regime, for every outdoor temperature t_{ext} considered.

An example of how the global COP varies with the discharge pressure and the subcooling degree is depicted in Fig. 2, where the outdoor temperature is equal to 36°C. Shown values are obtained by assuming $\varphi = 0.176$, as an average representative value of the cooling load ratio.

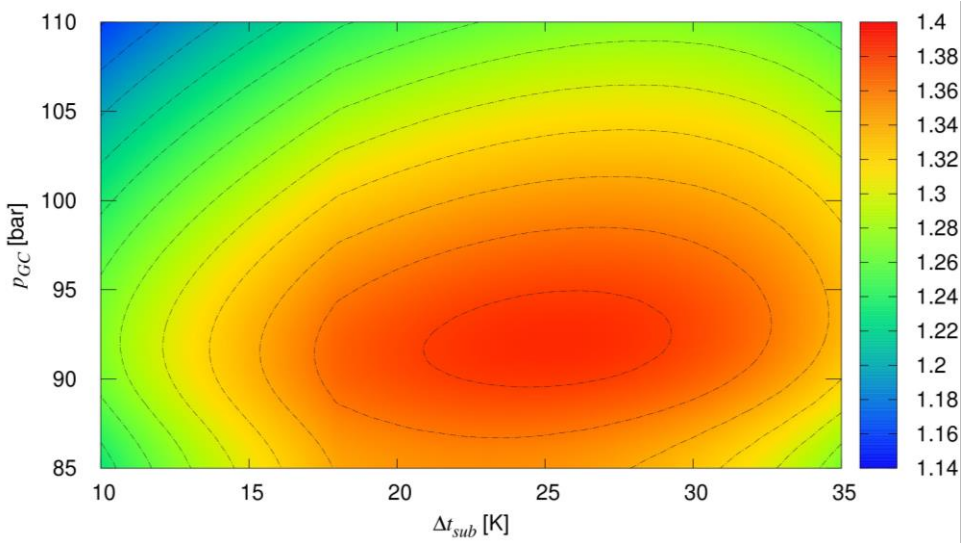


Figure 2: Overall plant COP colour map, against Δt_{sub} and p_{GC} , for outdoor temperature equal to 36°C and $\varphi = 0.176$.

Interpolation of the results of this last analysis leads to a polynomial expression, in terms of the subcooling degree Δt_{sub} and of t_{ext} , for the optimum gas cooler pressure, in transcritical regime, of the plant considered, and has the following form:

$$p_{GC}^{opt}(t_{ext}, \Delta t_{sub}) = c_1 t_{ext}^3 + c_2 \Delta t_{sub}^3 + c_3 t_{ext}^2 + c_4 \Delta t_{sub}^2 + c_5 t_{ext} + c_6 \Delta t_{sub} + c_7 t_{ext}^2 \Delta t_{sub} + c_8 t_{ext} \Delta t_{sub}^2 + c_9 t_{ext} \Delta t_{sub} \quad (6)$$

whose coefficients are:

$$\begin{aligned} c_1 &= 3.4333 \cdot 10^{-4} & c_2 &= -5.7308 \cdot 10^{-4} & c_3 &= -2.9695 \cdot 10^{-2} \\ c_4 &= -3.83115 \cdot 10^{-2} & c_5 &= 3.36129 & c_6 &= -2.7487 \cdot 10^{-1} \\ c_7 &= -2.24931 \cdot 10^{-3} & c_8 &= 2.32526 \cdot 10^{-3} & c_9 &= 5.98662 \cdot 10^{-2} \end{aligned}$$

and where the temperature values are in °C. The reduction of the gas cooler pressure Δp_{GC} allowed by the DMS, i.e. the difference between the discharge pressure without subcooling and the optimal value p_{GC}^{opt} (Eq. 6), is represented as colour map in Fig. 3 for the combination of subcooling degree and outdoor temperature values which is physically possible. The upper limit for the subcooling degree, which has been considered in the simulations, is imposed by the minimum subcooler outlet set point temperature $t_{sub, set}$ (5 °C) and depends on the external temperature through the gas cooler approach temperature difference. In Fig. 3, the contour lines of optimal gas cooler pressure p_{GC}^{opt} are also plotted. It can be noticed that the influence of the subcooling degree on the optimal value of the gas cooler pressure increases at higher outdoor temperature.

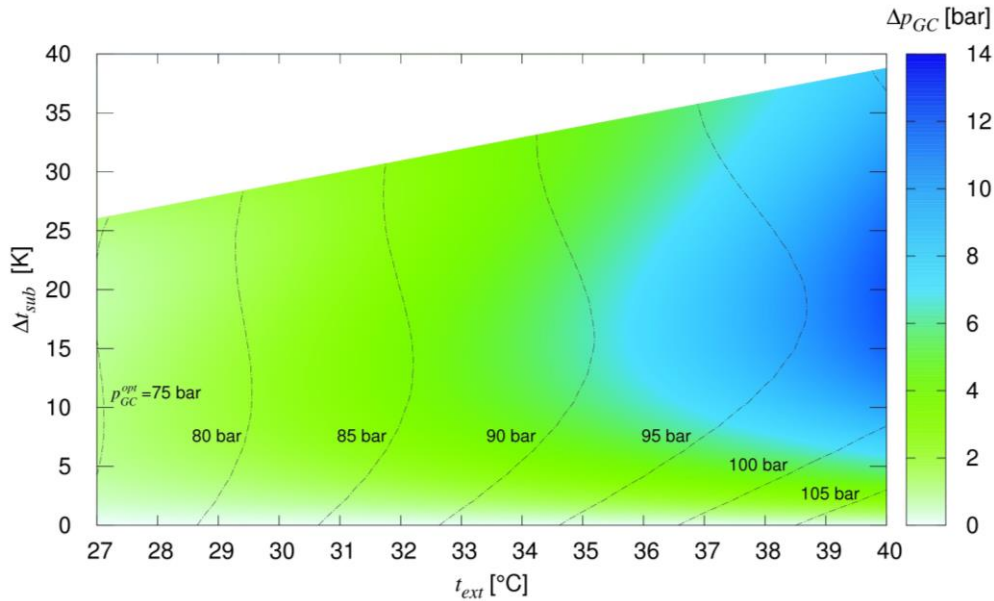


Figure 3: Achievable reduction of the gas cooler pressure colour map and optimal gas cooler pressure contour lines, against outdoor temperature and subcooling degree, $\phi = 0.176$.

4. ENERGY ANALYSIS

In this section, the results, in energy performance terms, of yearly based simulations are presented and discussed for a set of warm and hot climate conditions. The comprehensive model of the refrigeration system with DMS and the optimal control rule for the gas cooler pressure, both described in the previous sections, are used, with an hourly time step, to predict the annual electrical energy demand of the overall system. It is important to point out that the booster model includes the electrical demand for auxiliaries, which has been calibrated against monitored data and accounts on average around 3.2 kW [23]. As a consequence, a reduction of the COP with respect to the one of Eq. (3) is expected.

The outdoor temperature is time dependent as well as the cooling loads, from the display cabinets and cold rooms, which depend on the indoor conditions in terms of temperature and relative humidity.

The simulations are performed for a set of activation temperatures, subcooler set temperatures and α ratios (Table 1), in order to seek the best combination of such parameters for each climate condition considered.

4.1 Problem set

As already anticipated, the aim of the work presented in this section is to study how the annual energy performance of the CO₂ transcritical booster system combined with a R-1234yf DMS unit varies with the following main control parameters:

- Subcooler activation temperature t_{act} , indicates the temperature threshold, above its value the subcooler is activated. The minimum value considered is equal to 19°C, which is the lower limit of the transition zone [17];

- Subcooler outlet set temperature t_{set} , is the temperature that is aimed to achieve at the outlet of the subcooler, provided the cooling capacity of the DMS makes it possible.
- DMS cooling capacity Q_{sub} , expressed by the non-dimensional parameter α , defined as:

$$\alpha = \frac{Q_{sub}}{Q_{LT\ max} + Q_{MT\ max}} \quad (7)$$

which measures the ratio of the DMS cooling capacity itself to the maximum value of the refrigeration load elaborated by the main cycle.

An annual simulation has been run for all the possible combinations of the parameter sets reported in Table 1, which are:

- $t_{act} = 19, 22, 25$ °C;
- $t_{set} = 5, 10, 15, 20$ °C
- $\alpha = 25, 30, 35, 40, 45, 50$ %

The optimum gas cooler pressure is given by Eq. (6) both with and without subcooler. Eq. (6) has been obtained with $\varphi = 0.176$, which is a value very close to the average annual values at each operating condition considered; anyway it has been checked that the optimum gas cooler pressure changes less than 2.5 % in the whole range of φ values encountered in the simulations.

The minimum value for the subcooler outlet set point temperature $t_{sub,min}$ has been imposed equal to 5 °C, for the sake of guaranteeing a minimum vapour quality at the liquid receiver, so as to allow the operation of the flash gas valve and control the pressure at the intermediate value.

Regarding the climates considered in this study, four different weather locations, each corresponding to the Köppen-Geiger climate classification shown in Table 2, have been selected:

Table 2. Classification of the climate in the locations considered

Location	Country		Classification
Modena	Italy	Cfa	Humid, subtropical (Temperate, without dry season, hot summer)
Cairo	Egypt	BWh	Hot desert (Arid, desert, hot)
Bangalore	India	Aw	Tropical Savannah (Tropical, wet and dry)
Bangkok	Thailand	Aw	Tropical Savannah (Tropical, wet and dry)

The distributions of the outdoor air temperature at these locations, are represented in Fig. 4. It can be observed that, especially for Bangalore and Bangkok, most of the year is characterized by high outdoor temperature, with small variation among the seasons. In this kind of climate condition, DMS is exploited for most of the working hours. For instance, setting the activation temperature equal to 19°C, the DMS unit is active for 61.7% of the working hours in Cairo, 90.3% in Bangalore and 99.6% in Bangkok, while only for 35.9% in Modena. It must be underlined that Modena shows the widest temperature range, a peak temperature equal to 37°C, higher than Bangkok's maximum and a number of hours at 36 °C which is very similar to that of Bangkok climate.

As an improvement with respect to previous works [17, 18], both the LT and MT cooling loads are estimated separately at each climate considering the internal air temperature which on turn results from the dynamic thermal building simulation at the different outdoor conditions. The distribution of the total cooling load ($Q_{LT}+Q_{MT}$) of refrigerated display cabinets and cold rooms is reported in Fig. 5. During the opening hours the indoor temperature in the zone of refrigerated display cabinets is set to 20°C (with a minimum 15°C during the closing hours) when the outdoor temperature is lower than 15°C and it is set to not exceed 24°C. Thus the peak value of the cooling capacity is between 46 and 47 kW for all climates, whereas the distribution is obviously different. Bangkok climate presents the maximum frequency close to the peak value (more than 700 hours at 46 kW); the other climates present a maximum frequency around 60% of the peak value (27-29 kW);

the Bangalore climate presents another relative maximum around 80% of the peak value; Cairo and Modena have a larger range of operating conditions.

As a consequence, in the annual simulation the total cooling load and the cooling load ratio ϕ are changing independently hour by hour. Fluctuations in the cooling loads due to ambient conditions and operating conditions of the cabinets lead to some variability in the value of ϕ which can be estimated in Fig. 6.

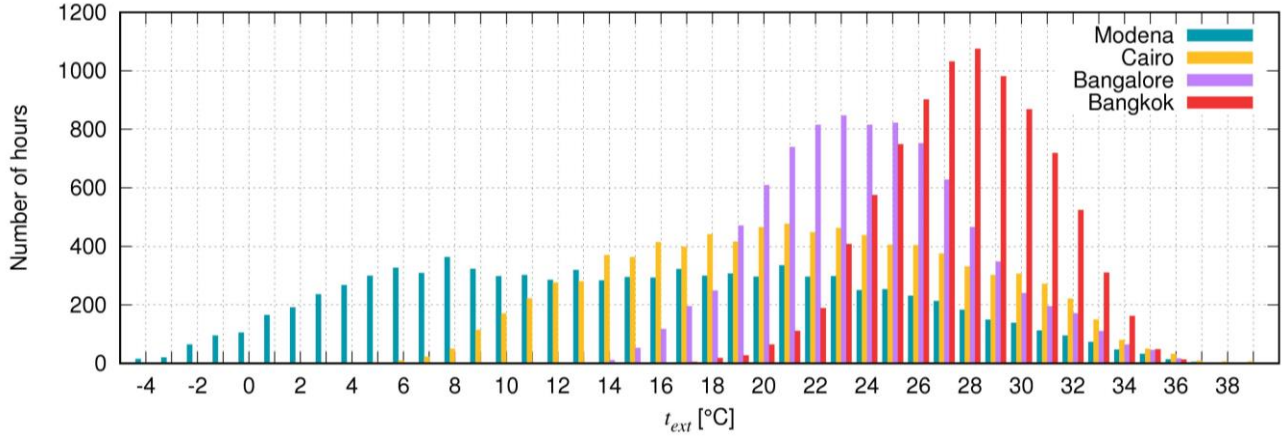


Figure 4: Temperature bins for the selected locations.

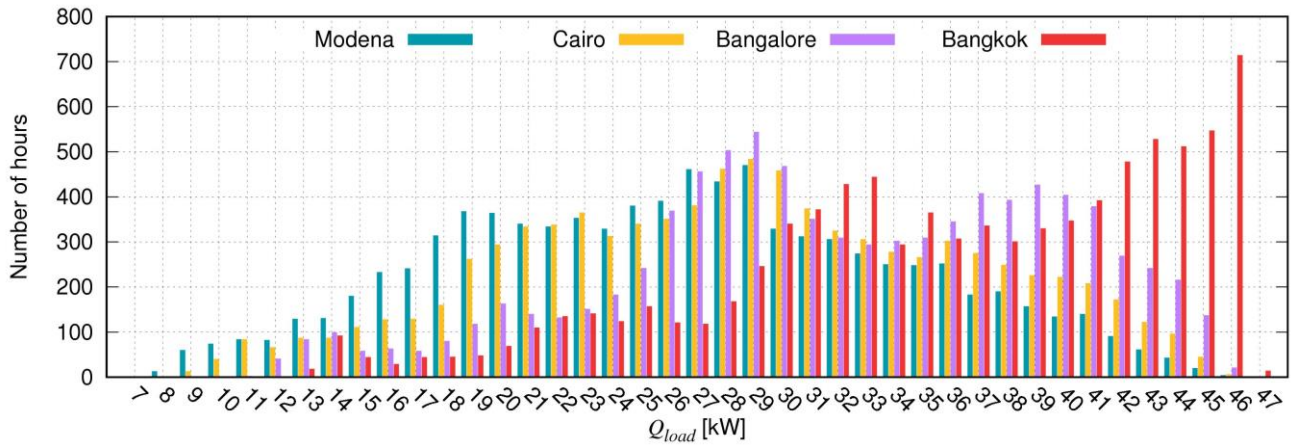


Figure 5: Cooling load bins for the selected locations.

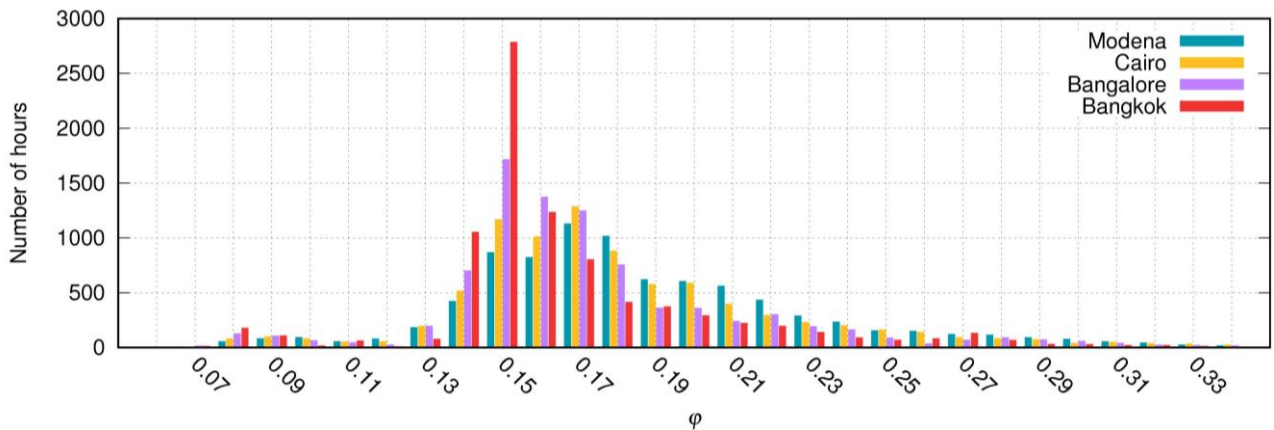


Figure 6: Cooling load ratio bins for the selected locations.

4.2 Results

The results are presented by comparing the total energy demand of a whole year for each case and climate. In particular, each calculation set contains every Q_{sub} in the α range for every couple ($t_{DMS, act}$, $t_{sub, set}$).

Given that the total peak cooling capacity of the considered system is almost the same for each climate, the value of Q_{sub} ranges for all locations in the same interval, from approximately 11.5 kW to 23.3 kW.

Simulations are carried out for a whole year with an hourly time step. The electrical energy utilization of the commercial refrigeration unit takes also into account the fraction needed for the plant auxiliaries. The final results are reported in terms of total energy use and of energy saving with respect to the basic booster system scheme B, which has a reference annual energy demand reported in Table 3.

Table 3. Annual energy demand for the booster system without DMS in the four selected climates.

Annual energy demand [MWh]	
Climate zone	Total
Modena	126.3
Cairo	158.6
Bangalore	181.4
Bangkok	229.9

As a start, Fig. 7 shows an example, for the climate conditions of Cairo, of how the set parameters affect the yearly energy demand of the CRU (Commercial Refrigeration Unit, i.e. the transcritical CO₂ booster system) on its own and of DMS separately.

As expected, the main tendency is that the power demand of the DMS grows with the size of the DMS itself, while the energy utilization of the CRU alone decreases. By lowering the activation temperature, the DMS demand increases and the CRU energy demand drops. As regards the influence of the outlet set temperature, there is the same tendency.

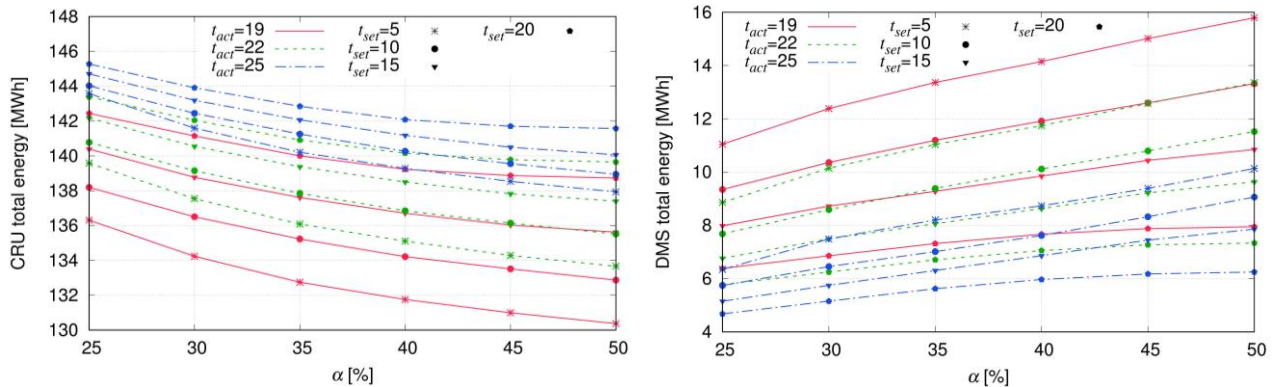


Figure 7: Yearly CRU energy demand and yearly DMS energy demand (right) in Cairo. Plots are shown for every combination of t_{act} , t_{set} and α .

In Fig. 8 the comprehensive results, in terms of energy saving, are shown for all the climates considered. It can be noticed that, for each solution set, an optimal size of the DMS exists with a corresponding value of α , that on average is between 35% and 45%. The choice of the correct DMS size is an important aspect, and the most suitable size should be evaluated also by economic considerations, as it will be done in the next section.

As regards the control rules we can infer that a t_{set} around 5°C or 10°C yields the best benefits for all climates with the exception of the hottest one where a t_{set} between 10°C and 15°C is recommended. High values of t_{set} , such as 20°C, have been explored but revealed to be much less effective. Furthermore, the lowest activation temperature t_{act} , equal to 19°C, is the best choice as it could have been expected. The hotter the weather, as the one of Bangkok for instance, the less the choice of t_{act} is significant, given that outdoor temperature is higher than t_{act} for the large part of the year (see Fig. 4). When we go to the DMS size, at mild climate conditions its choice is quite neutral, while when the climate of Bangkok is considered, a best choice appears.

In general terms, using the DMS at hotter climate conditions larger energy saving can be achieved, and the difference in saving between the most favourable choice and the least becomes more significant. A maximum value is present in almost every curve, proving that an optimal energy effective condition exists.

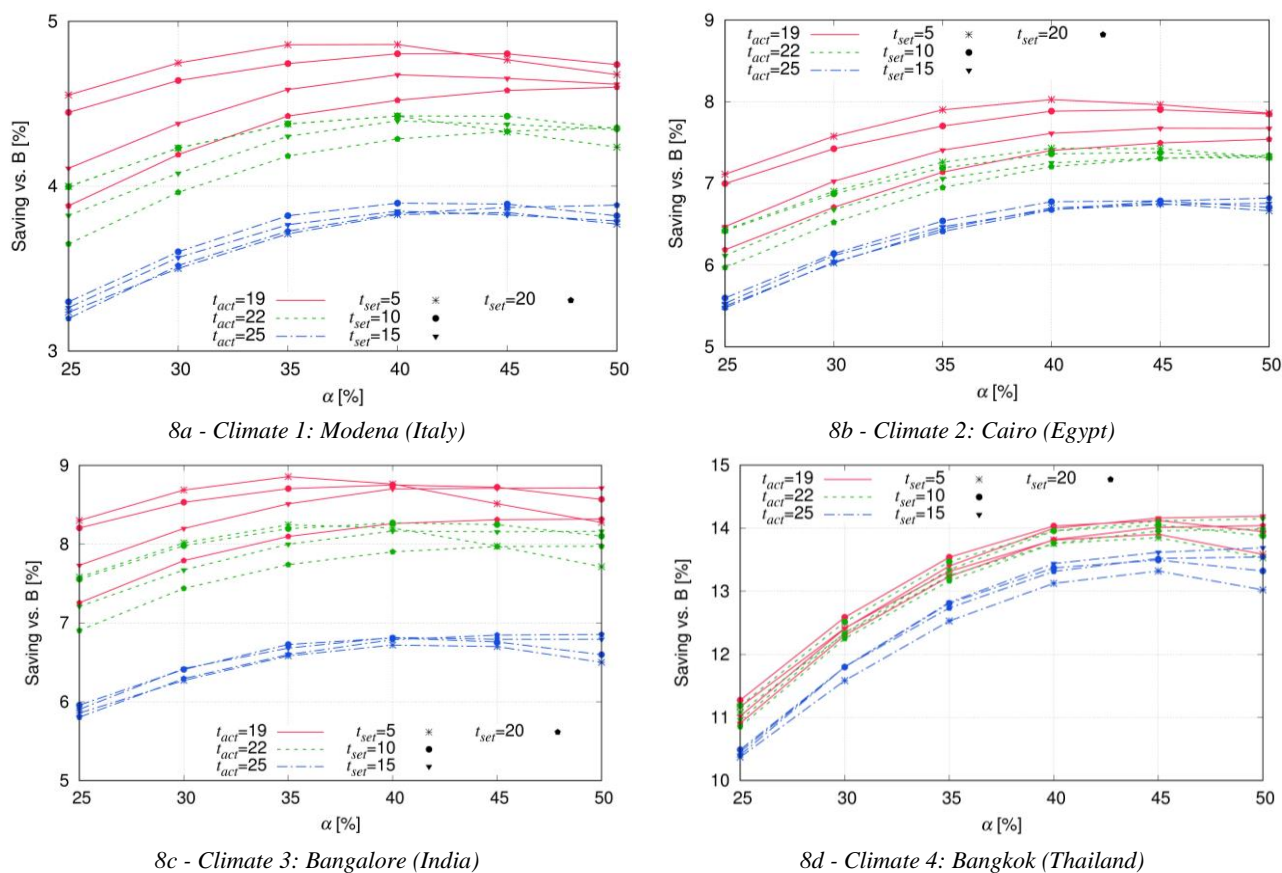


Figure 8: Yearly energy saving due to the use of DMS for each climate considered. Plots are shown for every combination of t_{act} , t_{set} and α .

An interesting result is, for each set of parameters, the percentage of operating hours of the DMS at which the subcooler set temperature t_{set} can be achieved, in order to give an idea of how close the system operates to the desired conditions. The subcooling degree is tightly related to the mass flow rate of refrigerant in the gas cooler line, and the higher it is the more difficult becomes to yield significant subcooling degrees, since the subcooling capacity of the DMS is constrained. As the load varies in time, many different subcooling degrees are obtained in the year, and the t_{set} value is not always achieved. Figure 9 shows an example, for mild and hot climate, of how frequently the subcooler outlet temperature meets the value imposed, at all the α values considered. Obviously for a given set (t_{act} , t_{set}), the higher the DMS size α the higher the number of hours the t_{set} can be achieved. For a given DMS size α , the percentage at which a certain t_{set} is achieved decreases at the increase of the activation temperature t_{act} : This reduction is more evident in the mild climate where the fraction of working hours at critical outdoor conditions is larger as t_{act} moves from 19° to 22°C and to 25°C, whereas in Bangkok climate (see Fig. 4) the number of hours with outdoor temperature in the range 19-22°C is a negligible fraction; thus the performance for cases (19, t_{set}) are much more similar to cases (22, t_{set}). Furthermore, in hotter climate the lowest t_{set} values are achieved with a lower frequency, whereas the highest t_{set} equal to 20 °C is approached nearly 100% hours by the largest DMS. This happens for all high t_{set} and α values when comparing Bangkok to Modena, and the reason is that the number of hours at very high outdoor temperature (> 35°C) is similar for the two climates (see Fig. 4), thus the number of hours at which the t_{set} is not achieved is also similar but less significant when compared to the total DMS working hours for Bangkok.

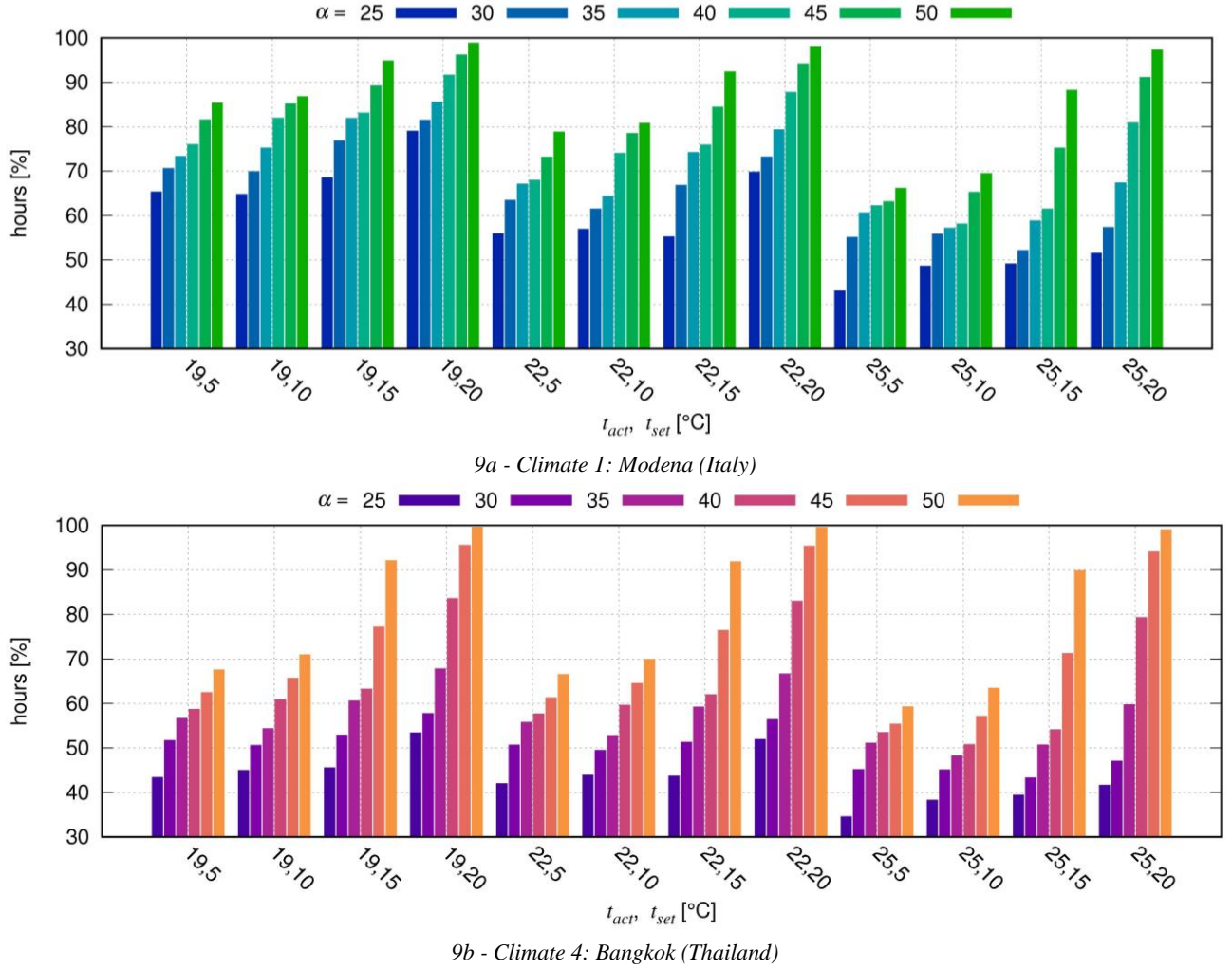


Figure 9: Number of hours, in percentage with respect to the DMS operating ones, when the t_{set} is achieved.

5. COST ANALYSIS

An energy analysis approach is useful when it comes to evaluate how to run a plant, in this case of study, in the most efficient way by finding the control rules, and schemes, that minimize the energy expense. However, such analysis is not adequate, on its own, at a design stage. Economic, or better cost considerations are indeed the most appropriate for this kind of task.

In this section, plant investment and running costs are applied to the results obtained in the previous chapter.

5.1 Plant costs

In this analysis, we focus only on the costs of the CRU and the DMS, while the refrigerated display cabinets and cold rooms, and their own piping, are not considered.

The CRU under exam, is composed by two compression stages, high stage and low stage, each consisting of two compressors, a master, driven by an inverter, and a slave. As already mentioned, the total maximum cooling load elaborated is 46.6 kW.

The heat exchange area of the gas cooler has been estimated to be around 23 m², and its cost is given by:

$$C_{GC} = 794A^{0.89} \text{ [€]} \quad (8)$$

where the exponent is taken from [26] and the constant is tuned on average actual costs in the Italian market. The cost of the other components plus all the sensors, valves and other equipment needed to make the CRU operative are summarized in Table 4.

Table 4. Cost of the plant components.

CO₂ booster system			
Component	Quantity	Single cost [€]	Cost [€]
LT compressors	2	1580	3160
MT compressors	2	6190	12380
Liquid receiver	1	4580	4580
Gas Cooler	1	12940	12940
Oil management	1	3245	3245
Safety system	1	4070	4070
Control valves	1	1140	1140
Sensors	1	495	495
Total plant components cost C_{plant}^{tot}			42010

The total amount of refrigerant required is approximately $m_{ref} = 140$ kg, with a leakage rate of 15% per year. The running costs are considered for a lifecycle of 10 years and are actualized by the following factor:

$$f = \frac{(1+i)^n - 1}{i(1+i)^n} \quad (9)$$

with an interest rate of 5% that yields an actualization factor f of 7.72. In Table 5 the running cost expressions are reported based on average costs for the refrigerant and for the electricity for Euro Area users in the band 20-500 MWh/y [27].

Table 5. Plant running specific costs and equations.

Description	Equation	Coefficient	Cost [€]
Maintenance	$C_m = e_m C_{plant}^{tot} f$	$e_m = 0.05$	16215
Refrigerant	$C_{ref} = m_{ref} c_{ref} (1+0.15f)$	$c_{ref} = 5.5$ [€/kg]	1662
Electricity [€/kWh]	$C_{el} = c_{el} W_{el,year} f$	$c_{el} = 0.19$ [€/kWh]	variable

Basically, the maintenance costs account for 5% of the total plant cost, the refrigerant cost is given by the initial cost plus the cost of the recharge and the electrical energy cost is a function of the total annual demand. As afore mentioned, each of the yearly costs is actualized by the factor f .

Up to this point, the only variable cost is the one of the electrical energy, as the plant scheme is always the same with different control rules.

As regards the DMS, a set of sizes have been taken into account, and the cost is considered a function of the cooling capacity of the compressor as by Eq. (10), [11, 25]:

$$C_{DMS} = 852Q^{0.46} \quad [€] \quad (10)$$

5.2 Results

Figure 10 shows the total cost to install and run the plant for its whole service life (10 years). Each curve is a function of the size of the DMS for a certain combination of t_{set} and t_{act} . The hotter the climate the more significant are the differences between the most favourable choice and the least. A minimum value is present in almost every curve, proving that an optimal cost effective condition exists.

Since the aim is to provide the guidelines to be followed at the design phase, as well as revealing the most favourable solution from an economic point of view, such optimal cost effective condition indicates the size

of the DMS and the control rules typical of a given climate.-The results in terms of cost analysis retrace those in terms of energy saving: optimal condition set (DMS size and control rules) is the same for both the energy and the cost analysis at all the climates considered. Thus the electrical energy cost has a higher impact on the definition of the optimal solution than the plant cost and ultimately than the DMS cost.

However, the total cost is not affected by large differences in the cases analysed. The saving given by the optimal solution compared to the worst one is around 1.1% in Modena, 1.9% in Cairo, 2.5% in Bangalore and 3.4 % in Bangkok. Furthermore, if we focus only on the size of the DMS unit, which is meant to be used by setting the optimal control rules, such difference is even smaller and becomes evident only at the hottest climate of Bangkok.

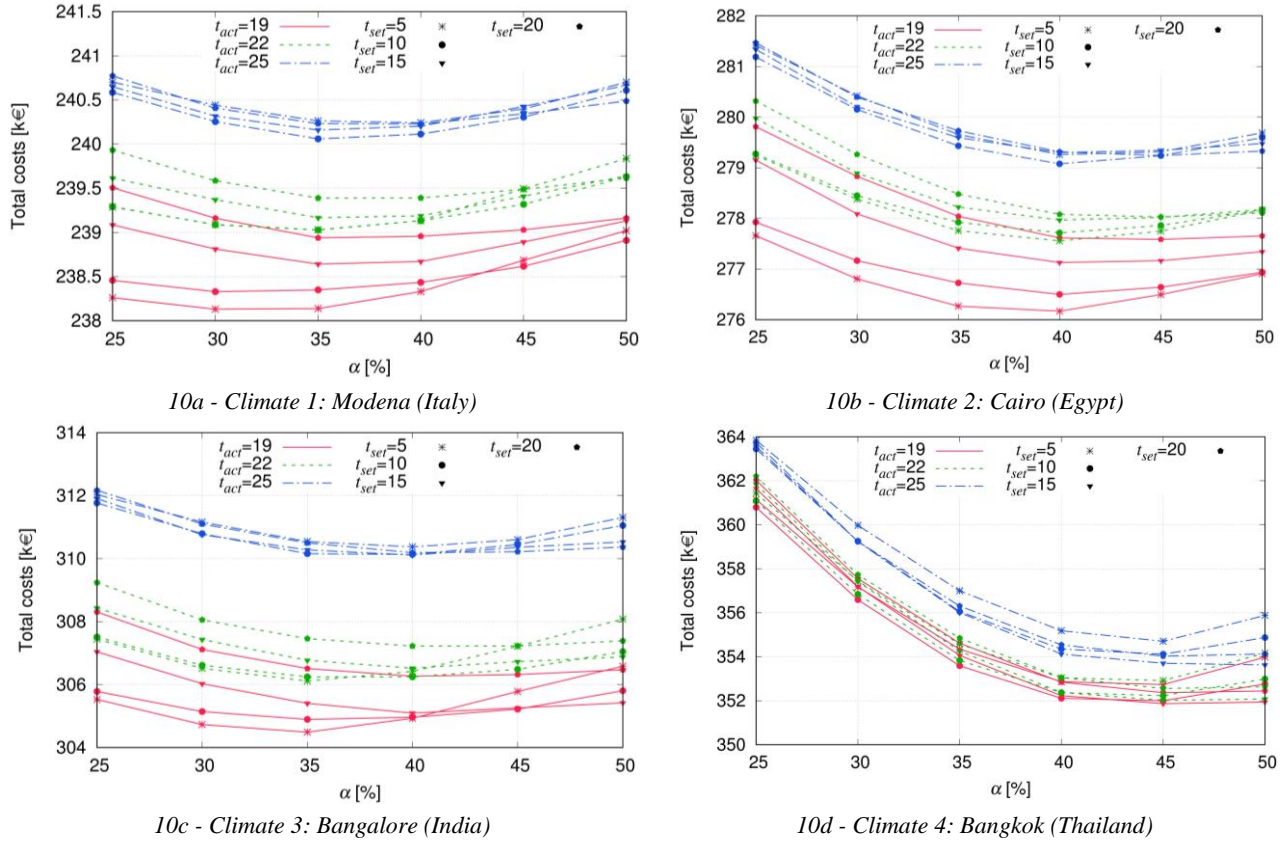


Figure 10: Total plant costs for a lifespan of 10 years, for each climate considered. Plots are shown for every combination of t_{act} , t_{set} and α .

Nevertheless, it is important to point out that the employment of the DMS itself leads to a significant cost saving if compared to the basic booster scheme without DMS. Table 6 shows the total cost comparison between the two solutions.

Table 6. Total cost of a plant without DMS and savings obtained using DMS at the optimal condition, for a 10-year life cycle.

Climate zone	Total cost without DMS [k€]	Saving with DMS [%]
Modena	250.6	4.9
Cairo	298.1	7.3
Bangalore	331.5	8.15
Bangkok	400.7	12.6

The employment of DMS leads to significant cost saving, especially when used in hot climates, if compared to the traditional booster system.

The analysis reveals that the size of the DMS does not affect much the investment that has to be made, even though the size indicated should be the correct choice. This is particularly true at the hottest climate conditions, where the size of the DMS plays an important role on the saving achievable. On the other climate conditions, the designer has to focus more on the optimal control rules which have been identified rather than on the DMS size, in order to operate the system in the most efficient way.

5. CONCLUSIONS

The use of Dedicated Mechanical Subcooling gives rise to the need of an optimisation process involving the gas cooler pressure, the subcooler activation and setpoint temperature values, the subcooling degree and the subcooler size, with the aim of improving the energy efficiency of the plant while considering costs.

A thermoeconomic analysis has been thus performed on the system considered, at four climate conditions from warm to hot, where subcooling is required. A variable refrigerating load annual profile has been estimated at each location depending on the operating conditions of display cabinets.

The results show that in terms of energy efficiency both an optimal size of the DMS and optimal control rules exist, whose effect changes with the climate. The best DMS size ranges from 35 to 45 % of the total cooling capacity; at mild – warm climates the influence of the DMS size is less significant and the energy saving changes in a 1 % range, while when hot climates are considered there can be a difference up to 3.5 % in the energy saving due to the DMS size. On the contrary, at mild-warm climates the control rules and particularly the activation temperature of the subcooler play a significant role, suggesting to activate the DMS at the lowest outdoor temperature here considered (19 °C) performing subcooling down to the lowest temperature suitable for the plant (5°C in this case). When varying the control rules, savings can change in a range of 2 % at mild-warm climates, 1 % in the hot one.

Finally, an economic analysis showed that the investment cost ranges from 13 to 20 % of the total cost in a 10 years life span, revealing that energy use is the most important cost item, and confirming the design and control rules previously identified.

ACKNOWLEDGMENT

The research leading to these results has received funding from the MIUR of Italy within the framework of the PRIN2017 project « The energy flexibility of enhanced heat pumps for the next generation of sustainable buildings (FLEXHEAT)», grant 2017KAAECT.

REFERENCES

- [1] Shecco, 2020. World guide to transcritical CO₂ refrigeration. <http://publication.shecco.com/publications/view/232>. [accessed 25/02/2021]
- [2] Llopis, R., Cabello, R., Sánchez, D., Torrella, E., 2015. Energy improvements of CO₂ transcritical refrigeration cycles using dedicated mechanical subcooling. *Int. J. Refrig.* 55, 129–141. <https://doi.org/10.1016/j.ijrefrig.2015.03.016>
- [3] Dai, B., Liu, S., Sun, Z., Ma, Y., 2017. Thermodynamic performance analysis of CO₂ transcritical refrigeration cycle assisted with mechanical subcooling. *Energy Proc.* 105, 2033–2038. <https://doi.org/10.1016/j.egypro.2017.03.579>
- [4] Llopis R., Nebot-Andrés L., Sánchez D., Catalán-Gil J., Cabello R., 2018. Subcooling methods for CO₂ refrigeration cycles. A Review. *Int. J. Refrig.*, 93, 85-107. <https://doi.org/10.1016/j.ijrefrig.2018.06.010>.
- [5] Llopis, R., Cabello, R., Sánchez, D., Torrella, E., 2015. Energy improvements of CO₂ transcritical refrigeration cycles using dedicated mechanical subcooling. *Int. J. Refrig.* 55, 129–141. <https://doi.org/10.1016/j.ijrefrig.2015.03.016>
- [6] Nebot-Andrés, L., Llopis, R., Sánchez, D., Cabello, R., 2016. Experimental evaluation of a dedicated mechanical subcooling system in a CO₂ transcritical refrigeration cycle. In: *Proc. 12th IIR Gustav Lorentzen Natural Working Fluids Conference, GL 2016*. Edinburgh (UK). *Refrig. Sci. Technol.* 965–972. <https://doi.org/10.18462/iir.gl.2016.1162>

- [7] Llopis R., Nebot-Andrés L., Cabello R., Sánchez D., Catalán-Gil J., 2016. Experimental evaluation of a CO₂ transcritical refrigeration plant with dedicated mechanical subcooling. *Int. J. Refrig.* 69, 361-368. <https://doi.org/10.1016/j.ijrefrig.2016.06.009>
- [8] Nebot-Andrés L., Sánchez D., Calleja-Anta D., Cabello R., Llopis R., 2021. Experimental determination of the optimum working conditions of a commercial transcritical CO₂ refrigeration plant with a R-152a dedicated mechanical subcooling, *Int. J. Refrig.*, 121, 258-268. <https://doi.org/10.1016/j.ijrefrig.2020.10.002>
- [9] Dai, B., Liu, S., Sun, Z., Ma, Y., 2017. Thermodynamic performance analysis of CO₂ transcritical refrigeration cycle assisted with mechanical subcooling. *Energy Proc.* 105, 2033–2038. <https://doi.org/10.1016/j.egypro.2017.03.579>
- [10] Bush J., Aute V., Radermacher R., 2018. Transient simulation of carbon dioxide booster refrigeration system with mechanical subcooler in demand response operation, *Science and Technology for the Built Environment*, 24:7, 687-699. <https://doi.org/10.1080/23744731.2017.1419733>
- [11] Mosaffa A.H., Garousi Farshi L., Infante Ferreira C.A., Rosen M.A., 2016. Exergoeconomic and environmental analyses of CO₂/NH₃ cascade refrigeration systems equipped with different types of flash tank intercoolers. *Energy Conversion and Management* 117, 442–453. <https://doi.org/10.1016/j.enconman.2016.03.053>
- [12] P. Gullo, B. Elmegaard, G. Cortella. Energetic, Exergetic and Exergoeconomic Analysis of CO₂ Refrigeration Systems Operating in Hot Climates. ECOS 2015 – 28th Int. Conf. on Efficiency, Cost, Optimization, Simulation and Environmental Impact of Energy Systems, June 2015, Pau (F).
- [13] Dai B., Zhao X., Liu S., Yang Q., Zhong D., Hao Y., Hao Y., 2020. Energetic, exergetic and exergoeconomic assessment of transcritical CO₂ reversible system combined with dedicated mechanical subcooling (DMS) for residential heating and cooling. *Energy Conversion and Management* 209 112594. <https://doi.org/10.1016/j.enconman.2020.112594>
- [14] Dai B., Qi H., Liu S., Ma M., Zhong Z., Li H., Song M., Sun Z., 2019. Evaluation of transcritical CO₂ heat pump system integrated with mechanical subcooling by utilizing energy, exergy and economic methodologies for residential heating. *Energy Conversion and Management* 192 202–220. <https://doi.org/10.1016/j.enconman.2019.03.094>
- [15] Mohammadi K., Powell K., 2020. Thermodynamic and economic analysis of different cogeneration and trigeneration systems based on carbon dioxide vapour compression refrigeration systems. *Applied Thermal Engineering* 164 (2020) 114503. <https://doi.org/10.1016/j.applthermaleng.2019.114503>
- [16] Cortella G., Coppola M.A., D'Agaro P., 2019. Subcooling with AC and Adiabatic Gas Cooling for Energy Efficiency Improvement: Field Tests and Modelling of CO₂ Booster Systems. In: Proc. 25th IIR Int. Congress of Refrigeration, ICR2019, Montreal, Canada, 3411-3418. <https://doi.org/10.18462/iir.icr.2019.784>
- [17] Cortella G., D'Agaro P., Coppola M.A., 2020. Transcritical CO₂ commercial refrigeration plant with adiabatic gas cooler and subcooling via HVAC: Field tests and modelling. *Int. J. Refrig.*, 111, 71-80. <https://doi.org/10.1016/j.ijrefrig.2019.11.022>
- [18] D'Agaro P., Coppola M.A., Cortella G., 2021. Effect of dedicated mechanical subcooler size and gas cooler pressure control on transcritical CO₂ booster systems. *Applied Thermal Engineering*, 182, 116145 <https://doi.org/10.1016/j.applthermaleng.2020.116145>
- [19] Klein, S.A., Beckman, W.A., Duffie, J.A., 2010. TRNSYS 17, A Transient System Simulation Program, Solar Energy Laboratory, University of Wisconsin, Madison, USA.
- [20] Polzot A., Gullo P., D'Agaro P., Cortella G., 2016. Performance Evaluation of a R744 Booster System for Supermarket Refrigeration, Heating and DHW. In: Proc. 12th IIR Gustav Lorentzen Natural Working Fluids Conference, GL 2016. Edinburgh (UK). *Refrig. Sci. Technol.* 2016, 154-161. <https://doi.org/10.18462/iir.gl.2016.1022>
- [21] Polzot A., D'Agaro P., Gullo P., Cortella G., 2016. Modelling commercial refrigeration systems coupled with water storage to improve energy efficiency and perform heat recovery. *Int. J. Refrig.*, 69, 313-323. <https://doi.org/10.1016/j.ijrefrig.2016.06.012>

- [22] Cortella G., D'Agaro P., Coppola M.A., 2018. Simulations and field tests of a CO₂ refrigerating plant for commercial refrigeration. In: Proc. 13th IIR Gustav Lorentzen Conference on Natural Refrigerants, Valencia (E). Refrig. Sci. Technol., (June 2018), 556-563. <https://doi.org/10.18462/iir.gl.2018.1215>
- [23] D'Agaro P., Coppola M.A., Cortella G., 2019. Field Tests, Model Validation and Performance of a CO₂ Commercial Refrigeration Plant Integrated with HVAC System. Int. J. Refrig., 100, 380-391, <https://doi.org/10.1016/j.ijrefrig.2019.01.030>
- [24] Bell, I.H, Wronski, J., Quoilin, S., Lemort, V., 2014. Pure and Pseudo-pure Fluid Thermophysical Property Evaluation and the Open-Source Thermophysical Property Library CoolProp. Ind. Eng. Chem. Res. 53(6), 2498-2508.
- [25] IPCC, Climate change 2013, The Physical Science Basis
- [26] Farsi A., Mohammadi S.M.Hojjat, Ameri M., 2016. An efficient combination of transcritical CO₂ refrigeration and multieffect desalination: Energy and economic analysis. Energy Conversion and Management 127 (2016) 561–575. <https://doi.org/10.1016/j.enconman.2016.09.038>
- [27] Eurostat: Electricity prices for non-household consumers - bi-annual data. <https://ec.europa.eu/eurostat/> [accessed 25/02/2020]